Depletion regions and electronic surface states in doped semiconductor superlattices

Jian Zhang and Sergio E. Ulloa
Department of Physics and Astronomy and Condensed Matter and Surface Sciences Program, Ohio University, Athens, Ohio 45701-2979
(Received 1 February 1988)

The electronic level structure of a type-I semiconductor superlattice such as GaAs/$Al_xGa_{1-x}As$ has been calculated self-consistently in a tight-binding envelope approximation. Fermi-level pinning due to defects at the ends of the superlattice gives rise to novel surfacelike states lying in electronic subband gaps and having localized eigenstates. Varying barrier transparency and modulation-doping density are shown to affect the location of these surface levels within the subband gap. Application of a gate voltage across the superlattice produces drastic changes in the level structure, including transitions from extended to localized behavior in some eigenstates concurrent to shifts in their energies. Sensitivity to gate voltage should yield a unique electrooptical response function in these systems.

I. INTRODUCTION

Research on synthesized semiconductor superlattices has attracted a great deal of attention. Various successful studies on these systems have revealed very interesting physical phenomena and led to the realization of new semiconductor devices.[1,2] A primary example of such a system is the superlattice fabricated from layers of GaAs alternating with doped layers of $Al_xGa_{1-x}As$. Since $Al_xGa_{1-x}As$ has a larger energy gap than GaAs, this configuration forms a so-called type-I superlattice, which can be viewed as a multiple-potential-well and barrier arrangement with electrons (or holes) confined in the well (GaAs) region. Recent improvements in growing techniques such as molecular-beam epitaxy have made possible the growth of high-quality GaAs/$Al_xGa_{1-x}As$ heterostructures with very abrupt interfaces and very thin layers. The superb structures so attained allow for careful control of the transparency of the potential barriers to carrier tunneling. This motion from layer to layer introduces dispersion in the perpendicular direction, which gives rise to an anisotropic three-dimensional electronic system with well-controlled characteristics.

The basic features of the electronic level structure in these systems are reasonably well understood using a simple Kronig-Penney model with properly chosen parameters, such as the layer thickness and alloy composition (which determines the potential barrier height).[3,4] This model produces electronic subbands (or "minibands") with bandwidths and effective masses in good agreement with experiment.[1] However, more realistically, the system is only composed of a few layers and cannot be strictly viewed as a periodic system, so that surface effects must be included in a detailed calculation of the electronic level structure. Moreover, defect states (due to the termination of layer growth at the top of superlattice, and generated by deep impurity states in substrate materials commonly used) provide a reservoir of electronic traps at the ends of the superlattice which strongly pins the Fermi level to the semiconductor midgap.[5] These midgap defect states trap nearby electrons and produce depletion regions at the top and bottom layers of the superlattice which affect the overall electronic level structure of the system. We have found surfacelike superlattice states with energies lying in the subband gaps in a fashion similar to localized defect states although extending over several constituent layers. These surface states peel off from the miniband continuum and are shown to be rather sensitive to the specific values of the tunneling coefficient and doping density. Most interestingly, we also show that the level structure changes drastically with the application of an electric field perpendicular to the layers via a gate voltage. The applied electric field can transform the localized surface states into Bloch-like extended states, accompanied by energy shifts towards the miniband continuum. This behavior provides for unique surface states with tunable extension which might conceivably be used to monitor mobilities at different positions across the superlattice structure. Moreover, it clearly suggests the possibility of using this arrangement to finely tune the far-infrared response of the system for novel electrooptical modulator devices.

In what follows we present self-consistent calculations of the energy-level structure in these superlattices and the associated charge distributions. Section II describes the tight-binding model used in the calculation and Sec. III presents results and discussion.

II. OUTLINE OF THE CALCULATION

A type-I superlattice such as $Al_xGa_{1-x}As$/GaAs can be viewed as a set of N potential wells attractive to electrons and separated by finite potential barriers.[6] In this calculation, a set of Wannier states centered on the different layers and belonging to the lowest electron miniband has been used to describe the envelope of the electronic wave function associated to the tunneling motion in the superlattice direction (z-axis direction).[7] This assumes that only the lowest miniband is occupied by doping electrons, which is appropriate for typical doping

densities. Consequently, the wave function corresponding to the nth eigenstate can be written as

$$\Phi_n(z)=\sum_{j=1}^{N} b_j^n \phi_j(z) , \quad (1)$$

where ϕ_j is the Wannier state associated with the jth layer. The corresponding Hamiltonian in a tight-binding approximation is given by

$$H_z=\sum_j (v_j C_j^\dagger C_j - tC_{j+1}^\dagger C_j - tC_j^\dagger C_{j+1}) , \quad (2)$$

where C_j is the destruction operator associated with the Wannier state ϕ_j, and t is the nearest-neighbor hopping matrix element. v_j is the self-consistent potential felt by the electrons which takes into account the electron–donor-ion and electron-electron interactions in a Hartree approximation, and it obeys Poisson's equation

$$v_{j+1}-2v_j+v_{j-1}=4\pi e^2 a(\rho_+ a-\rho_j)/\epsilon , \quad (3)$$

where ρ_+ is the positive-ion background density, ρ_j is the *areal* electron density of layer j, a is the superlattice period, and ϵ is the average dielectric constant of the system.[8] In order to incorporate the existence of the midgap states mentioned above, the boundary conditions complementary to Eq. (3) are chosen as

$$v_{N+1}=\mu+\delta \quad (4)$$

for the free end and

$$v_0=v_1+(v_{N+1}-\delta+\delta'-v_1)a/L \quad (5)$$

for the end attached to the substrate buffer. Here, v_0 and v_{N+1} represent the value of the potential function at points just outside the superlattice layers (v_1 through v_N), μ is the Fermi energy of the system, and L is the thickness of the impurity-free buffer region on which typical superlattices are grown. The constants δ and δ' fix the Fermi level to the end layers of the superlattice at about 0.9 eV below the edge of the conduction band of GaAs, corresponding to the binding energy of the defect states.[5]

On the other hand, the electronic in-plane motion can be treated in a simple effective-mass approximation $E(k_t)=\hbar^2 k_t^2/2m$ since nonparabolicity effects are expected to be negligible at the energies of interest. The total energy of the system is therefore given by $E(n,k_t)=E_n+E(k_t)$, where E_n is the eigenvalue of H_z, $H_z\Phi_n=E_n\Phi_n$. The surface electron density per layer ρ_j can be obtained from

$$\rho_j=(m/\pi\hbar^2)\sum_{n\,(\le n')} |b_j^n|^2 F((\mu-E_n)/\Gamma\sqrt{2}) , \quad (6)$$

where $E_{n'}$ is the eigenvalue below and nearest to μ, and the function $F(x)=(\Gamma/\sqrt{2})\{x[1+\mathrm{erf}(x)]-[1-\exp(-x^2)]/\sqrt{\pi}\}$ takes into consideration the impurity broadening of the energy levels via a Gaussian function of width Γ (erf is the usual error function). The thermal broadening of the energy levels has been neglected for simplicity and because at typical low temperatures $kT \ll \Gamma$ (the value $\Gamma=1$ meV is used in our calculation). Energy-level structures were calculated numerically by solving Eqs. (2)–(6) self-consistently.

We are also interested in the effect of a gate voltage applied across the superlattice, in the direction perpendicular to the layers (z direction). This voltage affects the extension and profile of the depletion regions at the ends of the superlattice and we show in the next section that this also drastically affects the electronic level structure of the whole system. We simulate the effect of a gate voltage by varying the value of the parameters δ and δ' above since they control the value of the potential at the edges of the superlattice. In the calculations presented here we have kept δ' fixed and only changed δ, modeling the application of a gate voltage to the free end of the superlattice with respect to the middle layers of the structure. The effective gate voltage is defined as $V_{\mathrm{gate}}=\delta_0-\delta$, where $\delta_0=1.6$ eV is the value for the unbiased system.[8]

Notice also that the choice of boundary conditions above allows the total electronic charge to vary self-consistently, according to the constraint imposed by keeping the Fermi level fixed. This is physically equivalent to assume electrical connections to an external charge reservoir which is the most common experimental arrangement.[9] It is also especially important in the case of the applied gate voltage since V_{gate} can completely empty or fill entire layers of the structure in order to maintain electrostatic equilibrium. These large charge variations affect the total level structure and produce very important energy shifts, as shown in the following section.

III. RESULTS AND DISCUSSION

One of the main advantages of synthesized semiconductor superlattices is the possibility of being able to carefully control their electronic properties over a wide range by varying a number of physical parameters. Figure 1 shows the level structure of a $GaAs/Al_xGa_{1-x}As$

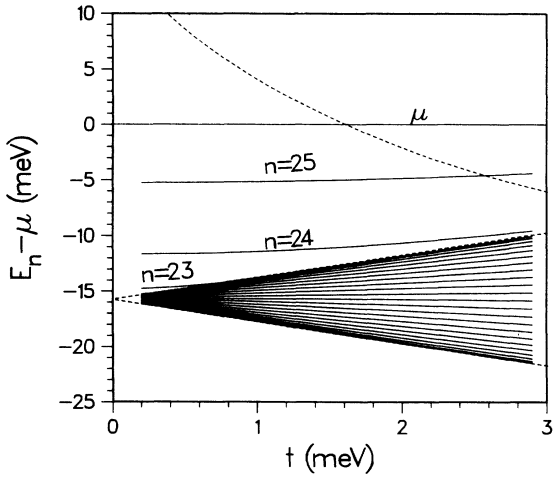

FIG. 1. z-motion electronic superlattice states for varying hopping parameter t, plotted with respect to Fermi level μ. Dashed lines denote edges of lowest two Kronig-Penney minibands. Notice midgap states, labeled with their n index.

superlattice with 30 periods and $\rho_+ = 1.9 \times 10^{17}$ cm^{-3}, as a function of the nearest-neighbor hopping parameter t. The z-motion eigenvalues E_n are plotted relative to the Fermi level μ in the region $t = 0.2$–2.9 meV which corresponds to easily accessible experimental values of alloy composition and layer thickness (notice that only centers of these Γ-broadened levels are shown).[3,4] As expected, the miniband is broadened for increasing values of t, equivalent to increasing transparency of the barriers [bandwidth $W = 4t$ in the case of the unperturbed ($v = 0$) tight-binding model]. However, a most remarkable feature of the level structure is the existence of "peel-off" states lying in the middle of the miniband gap, and corresponding in this figure to $n = 24$ and 25 (levels with $n \geq 26$ lie at higher energies, beyond the range shown in the figure). For reference, the edges of the unperturbed Kronig-Penney minibands for the same superlattice parameters appear as dashed lines in the figure.

The states which detach from the miniband continuum possess a surfacelike character in that their eigenfunctions are extremely localized within a few superlattice periods near the ends. The physical nature of these states can be understood in terms of the inhomogeneous self-consistent Coulomb potential appearing in the z-motion Hamiltonian. The resulting potential is rather flat within the middle superlattice layers and increases steeply near the ends of the chain since these regions correspond to the depletion zones. The larger value of the potential near the ends of the superlattice force a smaller overlap with layers in the middle of the structure which produces wave-function localization and correspondingly large eigenvalues. This also explains the insensitivity of the surfacelike states to changes in the transparency of the superlattice layers, since the values of the self-consistent potential in the region where the wave function is peaked are much higher than the individual potential barriers. On the other hand, the states in the miniband continuum which have wave functions extending over the large region of flat potential function are strongly affected by variations in t.

Notice also in Fig. 1 that the energy state E_{23} separates from the miniband only for small values of t, $t \lesssim 0.6$ meV. When clearly detached from the band, $t \simeq 0.2$ meV, its eigenvector exhibits surfacelike characteristics, being localized over five layers at the substrate end of the superlattice ($j \simeq 2$–6), and strongly peaked at layer $j = 3$ (see Fig. 2). However, for $t \simeq 0.6$ meV, E_{23} joins the miniband at the same time that its eigenvector becomes less peaked and decays slowly up to layer 14. Eventually, for $t \gtrsim 0.8$ meV, E_{23} becomes a Bloch-like state, extending over the whole superlattice chain. The energy state E_{24} has a similar behavior, approaching the miniband continuum for increasing t values. However, since it lies higher in energy, it is less affected by the transparency of the superlattice. Nevertheless, its eigenvector is localized near the free end of the superlattice and it evolves from being nonzero for $j \simeq 24$–28 at $t \simeq 0.2$ meV, to $j \simeq 16$–28 for $t \simeq 2.8$ meV.

We have also studied the effects of different doping levels on the electronic level structure. Figure 3 shows the resulting level configuration for increasing doping density

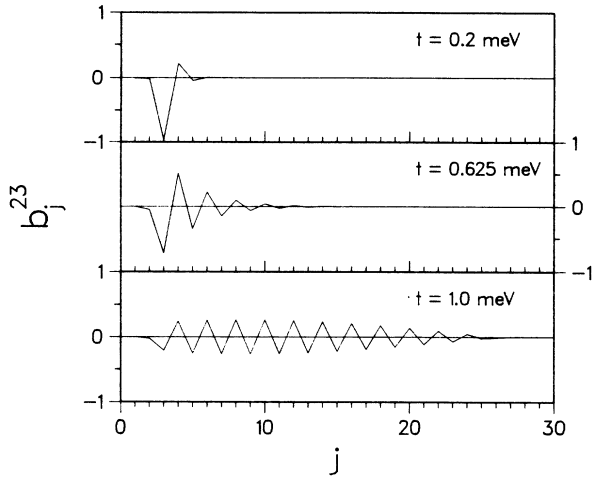

FIG. 2. Eigenvectors corresponding to E_{23} for different t values. Notice localized to extended transition for increasing t.

in a system with $t = 0.625$ meV. In this figure the energy levels are plotted with respect to the bottom of the miniband, and the corresponding Fermi energy μ appears as a dashed line. The most important feature here is the presence of two clearly developed surface states for all values of the doping density. These states are associated with each of the superlattice ends and change their surface character as the doping and corresponding electronic densities change. Indeed, one sees that as the population of a given level changes by shifting with respect to the Fermi level, other states rearrange in such a way as to always maintain a miniband-gap surface state. Consequently, states that are Bloch-like extended for some value of ρ_+, do change their eigenfunction to become highly localized about one end of the structure. Notice also that since the total negative charge changes (see Fig.

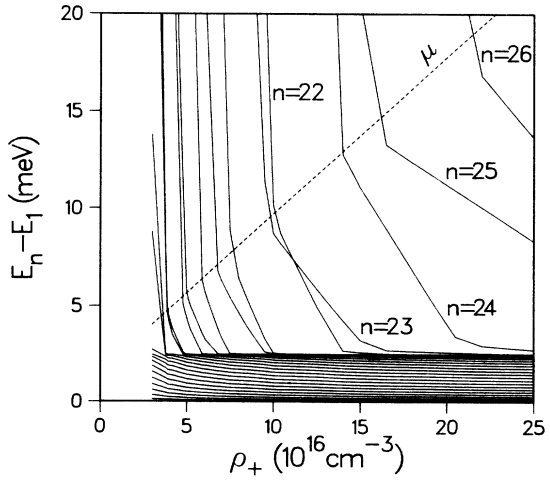

FIG. 3. Level structure for varying doping density ρ_+, and $t = 0.625$ meV. Levels plotted with respect to miniband bottom. Two clearly developed midgap surface states are always present. Fermi level appears dashed.

4), the effective extension of the depletion regions also changes, and the layer about which the surface state is localized shifts by one unit in the corresponding direction. Simultaneously, of course, the potential function is changing the extent of its flat region around the middle portion of the superlattice, with rather sharp slope near the ends. For small doping densities it is also clear that small changes produce large energy shifts since the potential function slopes even faster. All throughout these changes, the miniband continuum states are only slightly affected, slowly increasing their intervening separations in such a way as to keep the bandwidth $W \simeq 4t$.

Since the presence of depletion regions is associated with the surfacelike states presented above, it is only natural to expect that application of gate voltages would have an effect on the detailed position of the states and corresponding eigenfunctions. This would then allow us to fine tune the overall level structure of the superlattice in a continuous fashion. We have studied this aspect by modeling the application of a gate voltage to one end of the superlattice with respect to the middle of the structure, not unlike a modulation-doped field-effect transistor arrangement.[2,10] Figure 5 shows the resulting structure for $t=0.625$ meV and $\rho_+ = 1.9\times 10^{17}$ cm^{-3} versus the applied gate voltage $V_{\text{gate}} = \delta_0 - \delta$. Here, the eigenvalues are plotted with respect to the Fermi level μ. For increasing gate voltage, more and more levels are pulled below μ and the total negative charge in the system increases. As a given state moves down in energy, its eigenfunction changes character very rapidly from highly localized and surfacelike (when the eigenvalue is in the miniband gap), to extended Bloch-like (when the eigenvalue joins the continuum), in a fashion similar to that seen in Fig. 2 for varying t. This is accompanied by shifting of other levels which move to fill the place of the surface state, one of them always being below μ at each value of the voltage. The surface state E_{25} is insensitive to variations in the gate voltage since its eigenvector is associated with the bottom of the superlattice (peaked at $j \simeq 2-3$), and practically not affected by variations of the potential at the top layers of the structure. Figure 6

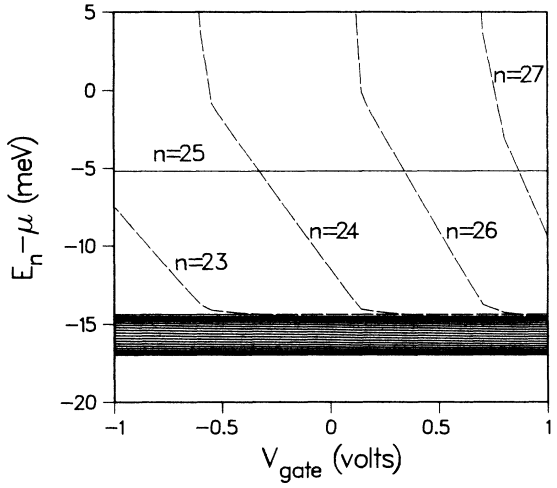

FIG. 5. Electronic levels vs gate voltage. Biasing of the system produces large shifts of the midgap states accompanied by changes in their wave-function localization.

shows the total electronic charge versus V_{gate} for the system of Fig. 5. Notice the linear dependence with rather sharp slope changes which occur every time a given level joins the miniband continuum and the occupation of the level above changes at a faster rate.

The sensitivity of the level structure to applied gate voltages should allow one to smoothly tune the electronic response of the system which would be very important in a number of experiments. In particular, we suggest an optical absorption experiment to directly probe the level structure, and especially the surfacelike states. The rather unusual tunable decay lengths of the surfacelike states should greatly affect the differential optical properties of the superlattice. This response could be used to construct a voltage-tunable far-infrared sensitive detector. Ongoing calculations of the optical response of the system will be presented elsewhere. The presence of these states is also expected to affect the plasmon dispersion re-

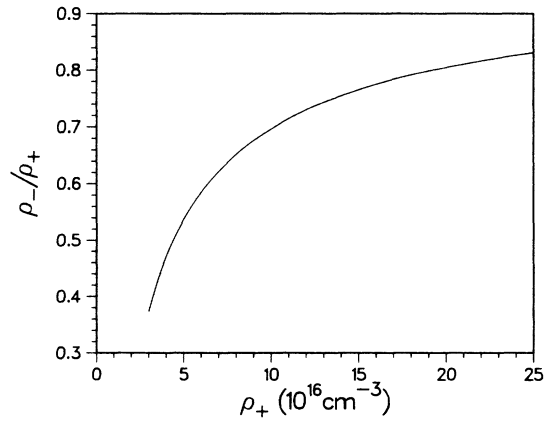

FIG. 4. Total electronic charge $\rho_- = (Na)^{-1}\sum_j \rho_j$ vs ion density ρ_+, corresponding to structure of Fig. 3.

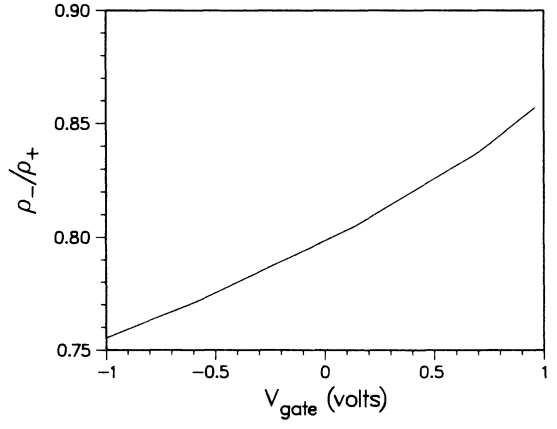

FIG. 6. Total charge density ρ_- vs V_{gate}. Sharp breaks in slope occur whenever a level leaves the band continuum in Fig. 5.

lations in these systems.[11] Similar states associated with the depletion regions have also been proposed to account for some features observed in recent quantum Hall effect experiments.[12,13] Indeed, the results presented here suggest the possibility of adjusting the alloy concentration depending on the layer position within the superlattice, in order to fine tune the position or even get rid of the surface states. This would locally change the effective hopping matrix element and may be desirable under some circumstances where depletion regions and these associated states are a further complication to an otherwise model system.

In conclusion, we have calculated the electronic level structure of a semiconductor superlattice as function of various experimentally accessible parameters such as the tunneling probability and the doping density. We have shown the unique properties of tunable surfacelike states with wave functions which extend over a rather large region. In particular, we studied the drastic changes of level structure with applied gate voltages. Far-infrared optical-absorption and plasmon experiments are suggested to directly probe these interesting features of the level structure in doped semiconductor superlattices.

ACKNOWLEDGMENTS

We would like to thank G. Kirczenow and H. J. Lozykowski for helpful discussions. This work was supported by the U.S. Department of Energy, Grant No. DE-FG02-87ER45334.

[1]L. Esaki, IEEE J. Quantum Electron. **22**, 1611 (1986), and references therein.

[2]H. Sakaki, IEEE J. Quantum Electron. **22**, 1845 (1986).

[3]See, for example, *Synthetic Modulated Structures*, edited by L. L. Chang and B. C. Giessen (Academic, New York, 1985).

[4]R. C. Miller, D. A. Kleinman, and A. C. Gossard, Phys. Rev. B **29**, 7085 (1984), and references therein.

[5]See, for example, *Proceedings of the Conference on Semi-Insulating III-V Materials, Kah-nee-ta, 1984*, edited by D. C. Look and J. S. Blakemore (Shiva, Nantwich, England, 1985), and references therein.

[6]For simplicity we concentrate on *n*-doped superlattices although the model can be generalized to treat hole systems as well.

[7]See, for example, J. Bleuse, G. Bastard, and P. Voisin, Phys. Rev. Lett. **60**, 220 (1988).

[8]Difference in the electronic effective mass across the two constituent semiconductors is neglected and we use the average dielectric constant. The various constants used in the calculation correspond to a 30-period GaAs-$Al_xGa_{1-x}As$ system: $m=0.067$, $\epsilon=12.5$, $a=226$ Å, $L=1100$ Å, $\delta=1.6$ eV, $\delta'=1.3$ eV, $\Gamma=1$ meV, and $N=30$.

[9]Interesting floating-gate experiments have also been performed, where the total electronic charge is kept constant. See R. T. Zeller, F. F. Fang, B. B. Goldberg, S. L. Wright, and P. J. Stiles, Phys. Rev. B **33**, 1529 (1986).

[10]H. L. Stormer, A. C. Gossard, and W. Wiegmann, Appl. Phys. Lett. **39**, 493 (1981).

[11]J. K. Jain and S. Das Sarma, Phys. Rev. B **35**, 918 (1987).

[12]H. L. Stormer, J. P. Eisenstein, A. C. Gossard, W. Wiegmann, and K. Baldwin, Phys. Rev. Lett. **56**, 85 (1986).

[13]S. E. Ulloa and G. Kirczenow, Phys. Rev. Lett. **57**, 2991 (1986).